Multifidelity Uncertainty Quantification for Optical Structures

Niklas Georg, Christian Lehmann, Ulrich Römer, and Rolf Schuhmann

Abstract This work addresses uncertainty quantification for optical structures. We decouple the propagation of uncertainties by combining local surrogate models with a scattering matrix approach, which is then embedded into a multifidelity Monte Carlo framework. The so obtained multifidelity method provides highly efficient estimators of statistical quantities jointly using different models of different fidelity and can handle many uncertain input parameters as well as large uncertainties. We address quasi-periodic optical structures and propose the efficient construction of low-fidelity models by polynomial surrogate modeling applied to unit cells. We recall the main notions of the multifidelity algorithm and illustrate it with a split ring resonator array simulation, serving as a benchmark for the study of optical structures. The numerical tests show speedups by orders of magnitude with respect to the standard Monte Carlo method.

1 Introduction

Manufacturing on the nanometer-scale exhibits strong variability in the finally built structures which should be addressed in a simulation based design approach. The field of uncertainty quantification provides suitable tools to model and quantify

N. Georg (✉)
Institut für Dynamik und Schwingungen, Technische Universität Braunschweig, Braunschweig, Germany

Centre for Computational Engineering, Technische Universität Darmstadt, Darmstadt, Germany
e-mail: n.georg@tu-braunschweig.de

C. Lehmann · R. Schuhmann
Theoretische Elektrotechnik, Technische Universität Berlin, Berlin, Germany
e-mail: lehmann@tet.tu-berlin.de; rolf.schuhmann@tu-berlin.de

U. Römer
Institut für Dynamik und Schwingungen, Technische Universität Braunschweig, Braunschweig, Germany
e-mail: u.roemer@tu-braunschweig.de

M. van Beurden et al. (eds.), *Scientific Computing in Electrical Engineering*,
Mathematics in Industry 36, https://doi.org/10.1007/978-3-030-84238-3_13

uncertainties in the geometrical and material constitutive parameters. In this contribution, we focus on the benchmark example of a split ring resonator (SRR) array with random input data. In particular, we model uncertainties in the SRR geometry with random variables and quantify the implied variation in the frequency response of the system. Such quasi-periodic optical structures may feature a large number of uncertain parameters which makes the application of many methods, such as standard or even sparse Polynomial Chaos difficult, see [1] for instance. We present a remedy by applying spectral polynomial expansions on the unit cell level in the framework of the Scattering Matrix Approach (SMA) [2], which yields a significant reduction of the computational effort. Since the coupled surrogate model may be biased, we use a Multifidelity Monte Carlo (MFMC) method [3], which combines different numerical models with different fidelity, to obtain efficient statistical estimators. In particular, through limited recurrences to a high-fidelity simulation of the entire structure, the MFMC method then corrects for possible approximation errors in the low-fidelity data.

2 Decoupled Uncertainty Propagation with Scattering Matrices

Our benchmark application is a simplified model of an array of coupled SRRs, motivated by the research on optical metamaterials [4, 5]. It consists of a periodic, but finite-size array of metallic SRR structures on a nanometer-scale, each of which can be interpreted as a realization of a resonance circuit, with the ring and the small gap acting as inductance and capacitance, respectively. More details on the geometry and setup will be given in Sect. 4. Due to the unavoidable tolerances in manufacturing of such small structures the geometric properties of each SRR will slightly vary, and the periodicity of the array of coupled resonator will not be perfect (see Figs. 54 and 57 in [5] for an illustration). Thus, we introduce a parameter vector $\mathbf{y}_{\text{cell},j} \in \Xi \subset \mathbb{R}^P$, which models variations in the geometry or material of the structure in cell j. The full input vector is then given as $\mathbf{y} = (\mathbf{y}_{\text{cell},1}^T, \ldots, \mathbf{y}_{\text{cell},N}^T)^T \subset \mathbb{R}^{N \cdot P}$, and all results of the forward model depend on this input vector.

The structure is excited by a plane wave and the reflection and transmission coefficients are evaluated. Translated into the language of dispersion analysis, the array is expected to feature a number of bandgaps, i.e. intervals on the frequency (or wavelength) axis where no transmission through the structure is possible. Both the finite size of the arrays (in our case up to seven unit cells) and the parameter variation in each SRR will have some influence on the corresponding limit frequencies.

The electromagnetic treatment of this application example requires the solution of the wave equation with an appropriate excitation at the ports. From the field solutions the amplitudes a_i and b_i of properly normalized incoming and outgoing waves are determined. They are coupled by the scattering matrix $\mathbf{S}(j\omega)$,

$$(\ldots b_i(j\omega)\ldots)^T = \mathbf{S}(j\omega)\ (\ldots a_i(j\omega)\ldots)^T,$$

with $r(j\omega) = S_{11}(j\omega)$ the reflection coefficient at the input port. Note that we omit the frequency dependency of $\mathbf{S}$ in the following to enhance the readability.

For the discretization we apply the efficient Finite Integration Technique (FIT) time-domain algorithm [6]. It relies on a three-dimensional Cartesian mesh and allows calculating broadband results with single transient simulation runs (using Discrete Fourier Transform on the signals). The calculation of scattering parameters proceeds in two steps: First, the two-dimensional eigenvalue problem of the port apertures is analyzed to obtain the field patterns and cutoff-frequencies of the so-called waveguide modes. Note that a lossfree model is considered here, and the array of SRRs is transversally terminated by perfect electric and magnetic boundary conditions. Second, these mode patterns and their well-known orthogonality properties are used to both excite the three-dimensional structure and to extract the amplitudes of the out-going waves at the ports. From one simulation run, one column of the scattering matrix can be obtained. For further details on the FIT we refer to the literature.

A technique to reduce the computational cost in the analysis of periodic structures is to decompose the SRR array into its single unit cells and to calculate separate scattering matrices $\mathbf{S}^{(i)}$ for each of them. The final concatenation of these single-cell results can be accomplished by switching to the transfer matrices $\mathbf{T}^{(i)}$ which map the wave amplitudes of the right hand side of each cell to the left hand side (rather than from input to output quantities as with $\mathbf{S}$). For a system with 2 ports:

$$\begin{pmatrix} b_1 \\ b_2 \end{pmatrix} = \mathbf{S} \begin{pmatrix} a_1 \\ a_2 \end{pmatrix} \quad \leftrightarrow \quad \begin{pmatrix} b_1 \\ a_1 \end{pmatrix} = \mathbf{T} \begin{pmatrix} a_2 \\ b_2 \end{pmatrix} \quad \text{with } \mathbf{T} = \begin{pmatrix} S_{12} - S_{11}S_{21}^{-1}S_{22} & S_{11}S_{21}^{-1} \\ -S_{21}^{-1}S_{22} & S_{21}^{-1} \end{pmatrix}.$$

Extended formulas for larger $\mathbf{S}$, $\mathbf{T}$, which take several port-modes into account, can easily be derived. Using transfer matrices, the total system behavior of N cells is simply given by a matrix multiplication $\mathbf{T} = \mathbf{T}^{(1)} \cdot \ldots \cdot \mathbf{T}^{(N)}$. This approach has been used previously in [2, 7] and is referred to as SMA.

This procedure has the intrinsic weakness that the coupling between the unit cells is not governed by a single waveguide mode alone, but an unknown number of higher modes may contribute. Of course, the coupling of modes at frequencies below their cutoff-frequency decreases rapidly with increasing spatial distance of the single SRRs. However, especially if there are resonances within the frequency range of interest (which clearly is the case for the SRRs as one of their working principles), this systematic error may become significant. In theory an extension of the SMA to an arbitrary number of coupling modes is straight-forward. However, the required number (and/or selection) of modes is sometimes hard to estimate a-priori, and the calculation of the extended transfer matrix increases the computational cost. Our approach removes any possible systematic error introduced in the coupling, by treating the SMA-based predictions as low-fidelity data and by correcting them with a couple of time domain solutions of the entire structure.

Non-intrusive Uncertainty Quantification (UQ) usually requires the repeated evaluation of the scattering matrices $\mathbf{S}(\mathbf{y})$ for different values of the inputs $\mathbf{y}$. Even with SMA the computational cost to evaluate a large number of sample points using the FIT might become prohibitive. Hence, we propose to construct a surrogate model for a unit cell of the periodic structure. In particular, we use a spectral collocation method, i.e. an approximation

$$\mathbf{S}^{(j)}(\mathbf{y}_{\text{cell},j}) \approx \mathbf{S}_{\text{uc};C}(\mathbf{y}_{\text{cell},j}) := \sum_{i=1}^{C} \mathbf{S}^{(j)}\big(\mathbf{y}_{\text{cell},j}^{(i)}\big)\Psi_i(\mathbf{y}_{\text{cell},j}) \tag{1}$$

where uc is short for unit cell and $j = 1, \ldots, N$ refers to an arbitrary unit cell of the structure. Also, $\{\mathbf{y}_{\text{cell},j}^{(i)}\}_{i=1}^{C} \subset \Xi$ denotes a set of collocation points, e.g. Chebyshev nodes, and Ψ_i denote the corresponding barycentric Lagrange polynomials. We emphasize that the same surrogate model is employed for all cells. It can be straightforwardly employed to obtain a surrogate of the full structure based on the SMA as (after transformation into $\mathbf{T}$ matrices)

$$\mathbf{T}(\mathbf{y}) \approx \mathbf{T}_C(\mathbf{y}) := \mathbf{T}_{\text{uc};C}(\mathbf{y}_{\text{cell},1}) \cdot \ldots \cdot \mathbf{T}_{\text{uc};C}(\mathbf{y}_{\text{cell},N}). \tag{2}$$

We also emphasize that (2) can be evaluated with negligible computational cost. In order to highlight the efficiency of the proposed combination of SMA and spectral surrogates for the unit cell, we give a few comments on the alternative approach, i.e. spectral approximation of the full structure. Due to spectral convergence properties, global polynomial approximations can be highly efficient, even up to a moderately large number of parameters (e.g., up to 10–20) using adaptive sparse approximations, see e.g. [1]. However, these methods still suffer from the so-called curse-of-dimensionality, i.e. the rapid growth of computational cost w.r.t. the number of parameters. As the full structure has a significant larger number of parameters, i.e. by a factor of N, this would quickly result in a very large number of simulation runs. Additionally, the computational cost for each model evaluation would also be significantly larger, when the full structure is considered instead of a single unit cell.

3 Multifidelity Monte Carlo

MFMC generalizes the multilevel Monte Carlo approach, which was recently used in [8] for a high-frequency application. MFMC simulation combines low-fidelity models of different kinds, without quantified model errors, into an efficient sampling framework. By sampling the high-fidelity model at least one time, the MFMC approach provides an unbiased estimator. Moreover, a low variance and hence, a low root-mean-square error, is realized through optimal model management and the resulting estimator is typically much more efficient than the standard Monte Carlo

(MC) estimator. The MFMC methodology was introduced in a series of papers [3, 9] and is now well-established. Hence, in the following we limit ourselves to the key aspects and refer to the literature for a more complete introduction into the field.

We adopt a probabilistic approach to represent uncertainty, where $\mathbf{y}$ represents a realization of a random vector $\mathbf{Y}$. Let $g(\mathbf{Y})$ denote an output quantity derived from the simulated frequency response. MC simulation is then based on a sample $\{\mathbf{Y}_i, g(\mathbf{Y}_i)\}_{i=1}^K$, which can be used to estimate for instance the mean value of the model output. The mean value approximation and its mean-square error read

$$\mathbb{E}[g(\mathbf{Y})] \approx \hat{g}_K := \frac{1}{K}\sum_{i=1}^{K} g(\mathbf{Y}_i), \qquad \mathbb{E}[|\mathbb{E}[g(\mathbf{Y})] - \hat{g}_K|^2] = \frac{\mathbb{V}[g(\mathbf{Y})]}{K}. \tag{3}$$

Following [9], we consider a model family $\{g^{(i)}\}_{i=1}^M$, where $g^{(1)}$ represents the high-fidelity model, and $g^{(i)}$ for $i \geq 2$ represent low-fidelity models, obtained for instance by SMA in combination with surrogate modeling. The MFMC estimator samples all models and combines the results into a single estimator as

$$\mathbb{E}[g] \approx \hat{g}_{\mathrm{MFMC}} = \hat{g}^{(1)}_{K^{(1)}} + \sum_{i=2}^{M} \alpha_i \left(\hat{g}^{(i)}_{K^{(i)}} - \hat{g}^{(i)}_{K^{(i-1)}}\right),$$

where $\hat{g}^{(i)}_{K^{(i)}}$ denotes the standard MC estimator based on the sample $\{\mathbf{Y}_j, g^{(i)}(\mathbf{Y}_j)\}_{j=1}^{K^{(i)}}$ and $0 < K^{(1)} \leq K^{(2)} \leq \ldots \leq K^{(M)}$.

In place of low-fidelity error control, the model management of MFMC employs the Pearson correlation coefficient $\rho_{1,i}$ between the high-fidelity model $g^{(1)}$ and the low-fidelity model $g^{(i)}$. In particular, low-fidelity models with a high $\rho_{1,j}$ and a low computational cost w_i are sampled extensively. For a given computational budget $\mathscr{B}$, MFMC minimizes the mean-square error by appropriately choosing α_i, $K^{(i)}$, see [9] for details. With $\sigma_i = \mathbb{V}[g^{(i)}(\mathbf{Y})]^{1/2}$, the resulting estimator is unbiased with a mean-square-error of

$$\mathbb{E}[|\hat{g}_{\mathrm{MFMC}} - \mathbb{E}[g(\mathbf{Y})]|^2] = \frac{\sigma_1^2}{K^{(1)}} + \sum_{i=2}^{M}\left(\frac{1}{K^{(i-1)}} - \frac{1}{K^{(i)}}\right)(\alpha_i^2\sigma_i^2 - 2\alpha_i\rho_{1,i}\sigma_1\sigma_i). \tag{4}$$

4 Numerical Examples

We apply the UQ methods presented in the previous section to the benchmark problem of an SRR array introduced in the beginning of Sect. 2. First, we give some details on the considered numerical models, before investigating the performance of the proposed UQ methodology.

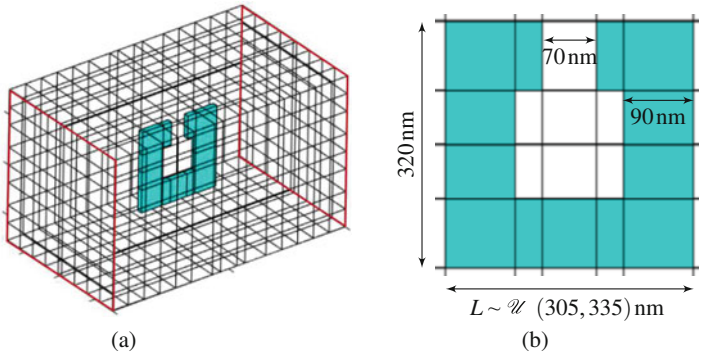

Fig. 1 Numerical model of SRR array. Depicted is only one cell out of seven. (**a**) Unit cell of size 1 µm × 0.6 µm × 0.6 µm. Red boundaries indicate the ports. (**b**) Geometry specification. Thickness: 20 nm. Uncertain longitudinal length L of SRR element

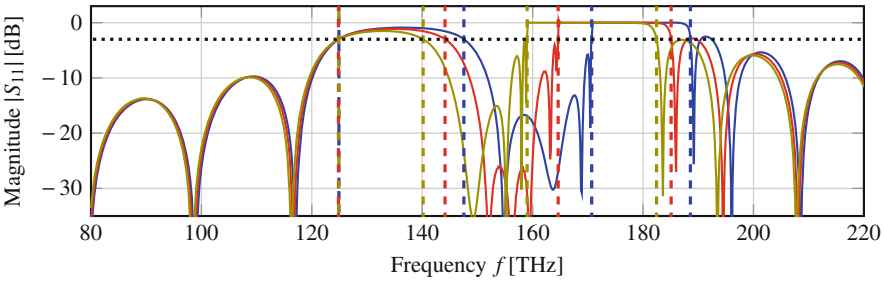

Fig. 2 Broadband scattering parameter for different realizations of SRR array. Dashed vertical lines indicate respective limit frequencies of considered bandgaps. Dotted line refers to −3 dB line

We consider a SRR array with $N = 7$ cells. The employed Cartesian grid as well as the geometric dimensions (taken from [4], except for the enlarged cell size) are presented in Fig. 1, where we consider an uncertain longitudinal length $L^{(j)}$ of each SRR element in the range of 320 nm ± 15 nm. Hence, the random vector $\mathbf{Y}$ is given as $(L^{(1)}, \ldots, L^{(N)})^T$, where $L^{(j)}$, $j = 1, \ldots, N$ are assumed to be independent and identically uniformly distributed. Figure 2 presents a broadband scattering parameter, in particular the fundamental reflection coefficient $|S_{11}|$, for different realizations of the structure. Two bandgaps can be observed, which can be defined by their limit frequencies, where the scattering parameter drops below −3 dB. The corresponding bandwidths b_i and center frequencies $f_{c,i}$, where $i \in \{1, 2\}$ refers to the first or second bandgap, can be computed from S_{11} in a post-processing step. For brevity, we restrict ourselves to the computation of the mean value of the center frequencies $\mathbb{E}[f_{c,i}]$ in the following. However, very similar findings hold for the bandwidths b_i as well. We further note that for some parameter sample points some additional resonances within the second bandgap appear which are due to the slightly detuned resonances in the series of SRRs. This effect is ignored in

Table 1 Employed numerical models of SRR array for MFMC study. The last two columns show the estimated correlation coefficients for both bandgaps

Symbol	Model	Cost w_i	$\rho_{1,i}$ for $f_{c,1}$	$\rho_{1,i}$ for $f_{c,2}$
$g^{(1)}$	Full model (FIT, $2 \cdot 10^5$ time-steps)	197.50 s	1.000000	1.000000
$g^{(2)}$	Full model (FIT, $2 \cdot 10^4$ time-steps)	11.25 s	0.999236	0.998035
$g^{(3)}$	SMA (FIT, 1 port-mode)	9.64 s	0.999943	0.968376
$g^{(4)}$	SMA (FIT, 2 port-modes)	115.47 s	0.999998	0.999998
$g^{(5)}$	SMA + unit cell surrogate (1 port-mode)	0.006 s	0.999943	0.967540
$g^{(6)}$	SMA + unit cell surrogate (2 port-modes)	0.026 s	0.999998	0.999886

the following evaluation of the MLMC algorithm and only the outer limits of this bandgap are considered.

An overview of the employed numerical models as well as the corresponding computational costs (measured in computation time for an in-house MATLAB implementation on a standard workstation) is given in Table 1. For the full FIT model $g^{(1)}$ we terminate the time stepping procedure if either the energy decays to -120 dB or a maximum number of $2 \cdot 10^5$ time-steps is reached. The low-fidelity model $g^{(2)}$ is obtained by restricting the maximum number of time-steps to $2 \cdot 10^4$. The low-fidelity models $g^{(3)}$ and $g^{(4)}$ are obtained by the SMA approach. For $g^{(3)}$ only the propagating fundamental TEM mode is considered, while $g^{(4)}$ additionally takes the evanescent first TM mode into account. The selection of suitable models is based on a pilot run (with a small sample) and model selection techniques, see also [3, 9].

The construction of the respective unit cell surrogate models for $g^{(5)}$ and $g^{(6)}$ in the offline-phase is based on $C = 7$ Chebyshev nodes, which are well-established non-equidistant interpolation nodes. Note that other choices are equally feasible, Gauss-Legendre nodes for instance. Surrogate modeling requires some additional computational effort, which, however, only needs to be invested once. Also, in this case, even a single model evaluation of $g^{(1)}$ requires a larger computational effort than constructing the surrogate models. Hence, we will neglect this cost here, for simplicity. We further note that the evaluation times of all models scale approximately linear w.r.t. to an eventually increased number of cells N, while the offline-cost for the surrogate models is independent of N. Accordingly, similar MFMC results, as presented in the following for $N = 7$, are also expected for SRR arrays with a different number of cells. Exemplarily, this has been confirmed for $N = 14$ numerically. However, we note that for larger models some care has to be taken regarding the concatenation within the SMA, since the multiplication of transfer matrices can become numerically unstable.

In order to evaluate the performance of the proposed methodology for the considered benchmark problem, we draw an input sample $\{\mathbf{Y}_i\}_{i=1}^{\tilde{K}}$ of size $\tilde{K} = 500$ and employ each model $g^{(j)}$ to compute the corresponding output samples $\{g^{(j)}(\mathbf{Y}_i)\}_{i=1}^{\tilde{K}}$, $j = 1, \ldots, 6$. The correlation coefficients with the high-fidelity

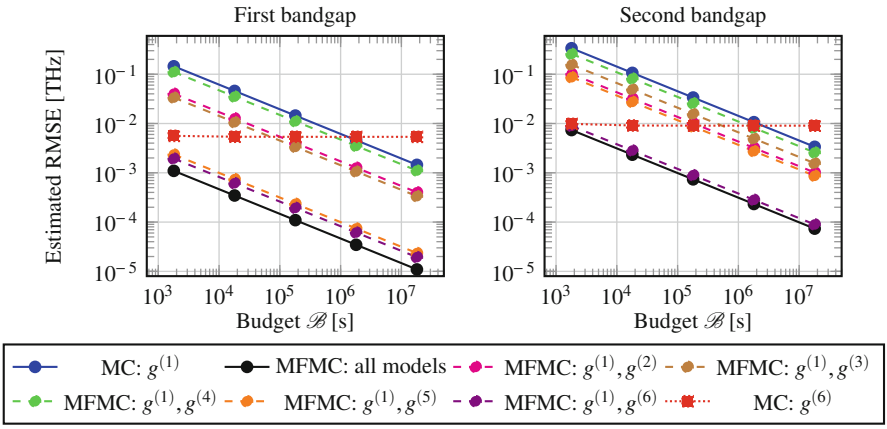

Fig. 3 Estimated RMSE for different MC and MFMC variants, see Table 1

model $g^{(1)}$ are then estimated as shown in Table 1. It can be observed that all low-fidelity models show a strong correlation with the high-fidelity model.

We employ an MFMC implementation which is based on the open-source Matlab library github.com/pehersto/mfmc, see [9]. In the following, we will compare the root-mean-square-errors (RMSEs) of MC and MFMC for given computational budgets $\mathscr{B}$, which can both be accurately estimated based on the samples $\{g^{(j)}(\mathbf{Y}_i)\}_{i=1}^{\tilde{K}}$, as explained in the following. The RMSE of standard MC on the high-fidelity model $g^{(1)}$ is obtained by (3), where K is given by $\frac{\mathscr{B}}{w_1}$ and the variance is replaced by the MC estimate for the variance using $\{g^{(1)}(\mathbf{Y}_i)\}_{i=1}^{\tilde{K}}$. This is shown in Fig. 3 in blue color. Similarly, the RMSE of MFMC can be estimated according to (4), as shown in black color in Fig. 3. We note that the proposed approach yields speedups by several orders of magnitude w.r.t. standard MC (for a fixed accuracy).

We note that the MFMC algorithm sorts out some models, as, for example, $g^{(2)}$ and $g^{(3)}$ have a smaller correlation with the high-fidelity model than the surrogate model $g^{(6)}$ but a higher computational cost. For completeness, we additionally show the convergence of MFMC using only $g^{(1)}$ and $g^{(j)}$, $j \in \{2, \ldots, 6\}$ with dashed lines in Fig. 3. As expected, in all cases this approach performs better than MC but worse than the combination of models chosen by the MFMC algorithm. It can be observed that, for both bandgaps, mainly the proposed unit cell surrogate models lead to the tremendous efficiency gains. While for the first bandgap considering only one port-mode could also be sufficient, for the second bandgap it is clearly necessary to consider two port-modes for the SMA. This is expected as the first bandgap is mainly governed by the fundamental resonance of the SRRs itself, whereas for the second one the mutual coupling between the cells play a larger role.

Finally, we show that the high-fidelity model evaluations within the MFMC framework are indeed required to remove the biasing error. If one would apply a standard MC method on the surrogate model $g^{(6)}$ solely (instead of $g^{(1)}$)

the associated error is represented by the dotted red line in Fig. 3. Both error contributions, the sampling and the biasing error, are estimated again with a Monte Carlo sample.

5 Conclusions

We have presented an uncertainty propagation technique for quasi-periodic optical structures with random influences, which combines surrogate modeling of unit cells, SMA and MFMC. The resulting multifidelity approach can significantly improve the efficiency of Monte Carlo sampling. In particular speedups by orders of magnitude were obtained for a split ring resonator. The proposed method exhaustively samples unit cell models which are combined through the scattering matrix approach and hence, can be evaluated efficiently. Only a single unit cell surrogate was required which significantly reduced the number of uncertain parameters and hence, the computational complexity. The surrogate-SMA data was then corrected with a few time domain simulations of the entire structure to obtain unbiased estimates of the bandgap properties.

Acknowledgments The work of Niklas Georg is supported by the DFG grant RO4937/1-1, the *Excellence Initiative* of the German Federal and State Governments and the Graduate School of Computational Engineering at TU Darmstadt. Christian Lehmann's work is funded by the DFG grant SCHU1157/11-1.

References

1. N. Georg, D. Loukrezis, U. Römer, S. Schöps, Enhanced adaptive surrogate models with applications in uncertainty quantification for nanoplasmonics. Int. J. Uncertain. Quan. **10**(2), 165–193 (2020)
2. B. Bandlow, R. Schuhmann, G. Lubkowski, T. Weiland, Analysis of single-cell modeling of periodic metamaterial structures. IEEE Trans. Magn. **44**(6), 1662–1665 (2008)
3. B. Peherstorfer, K. Willcox, M. Gunzburger, Survey of multifidelity methods in uncertainty propagation, inference, and optimization. SIAM Rev. **60**(3), 550–591 (2018)
4. S. Linden, C. Enkrich, M. Wegener, J. Zhou, T. Koschny, C. Soukoulis, Magnetic response of metamaterials at 100 Terahertz. Science **306**, 1351–1353 (2004)
5. K. Busch, G. von Freymann, S. Linden, S. Mingaleev, L. Tkeshelashvili, M. Wegener, Periodic nanostructures for photonics. Phys. Rep. **444**(3–6), 101–202 (2007)
6. T. Weiland, Time domain electromagnetic field computation with finite difference methods. Int. J. Numer. Model. El. **9**(4), 295–319 (1996)
7. H. Glock, K. Rothemund, U. van Rienen, CSC - A procedure for coupled S-parameter calculations. IEEE Trans. Magn. **38**(2), 1173–1176 (2002)
8. A. Litvinenko, A. Yucel, H. Bagci, J. Oppelstrup, E. Michielssen, R. Tempone, Computation of electromagnetic fields scattered from objects with uncertain shapes using multilevel Monte Carlo method. IEEE J. Multiscale Multiphys. Comput. Tech. **4**, 37–50 (2019)
9. B. Peherstorfer, K. Willcox, M. Gunzburger, Optimal model management for multifidelity Monte Carlo estimation. SIAM J. Sci. Comput. **38**(5), A3163–A3194 (2016)